

Aromatic hydrocarbon receptor-driven *Bax* gene expression is required for premature ovarian failure caused by biohazardous environmental chemicals

Tiina Matikainen¹, Gloria I. Perez¹, Andrea Jurisicova^{1,2}, James K. Pru¹, Jennifer J. Schlezinger³, Heui-Young Ryu³, Jarmo Laine⁴, Toshiyuki Sakai⁵, Stanley J. Korsmeyer⁶, Robert F. Casper², David H. Sherr³ & Jonathan L. Tilly¹

Published online: 16 July 2001, DOI: 10.1038/ng575

Polycyclic aromatic hydrocarbons (PAHs) are toxic chemicals released into the environment by fossil fuel combustion. Moreover, a primary route of human exposure to PAHs is tobacco smoke^{1,2}. Oocyte destruction and ovarian failure occur in PAH-treated mice^{1,2}, and cigarette smoking causes early menopause in women^{1,3}. In many cells, PAHs activate the aromatic hydrocarbon receptor (Ahr), a member of the Per-Arnt-Sim family of transcription factors^{4,5}. The Ahr is also activated by dioxin, one of the most intensively studied environmental contaminants. Here we show that an exposure of mice to PAHs induces the expression of *Bax* in oocytes⁶, followed by apoptosis. Ovarian damage caused by PAHs is prevented by *Ahr* or

Bax inactivation. Oocytes microinjected with a *Bax* promoter-reporter construct show Ahr-dependent transcriptional activation after PAH, but not dioxin, treatment, consistent with findings that dioxin is not cytotoxic to oocytes. This difference in the action of PAHs versus dioxin is conveyed by a single base pair flanking each Ahr response element in the *Bax* promoter. Oocytes in human ovarian biopsies grafted into immunodeficient mice also accumulate *Bax* and undergo apoptosis after PAH exposure *in vivo*. Thus, Ahr-driven *Bax* transcription is a novel and evolutionarily conserved cell-death signaling pathway responsible for environmental toxicant-induced ovarian failure.

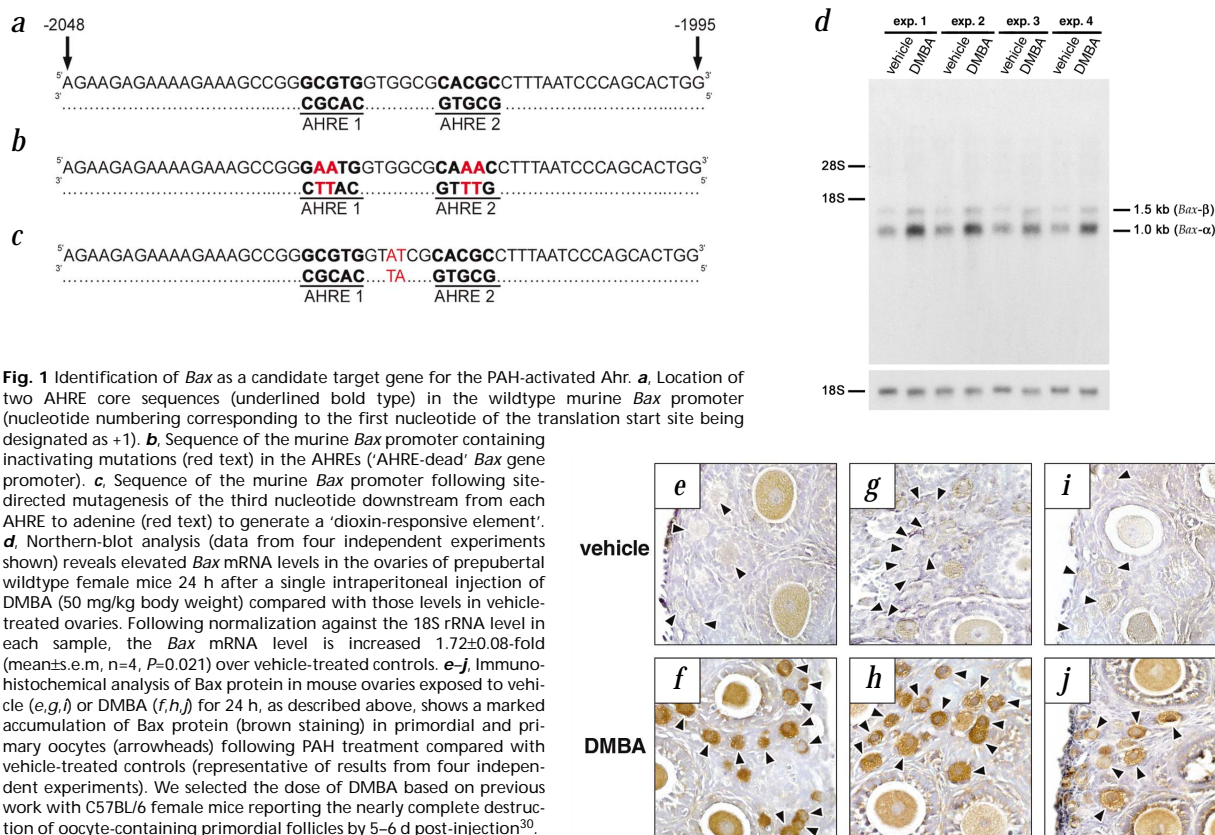
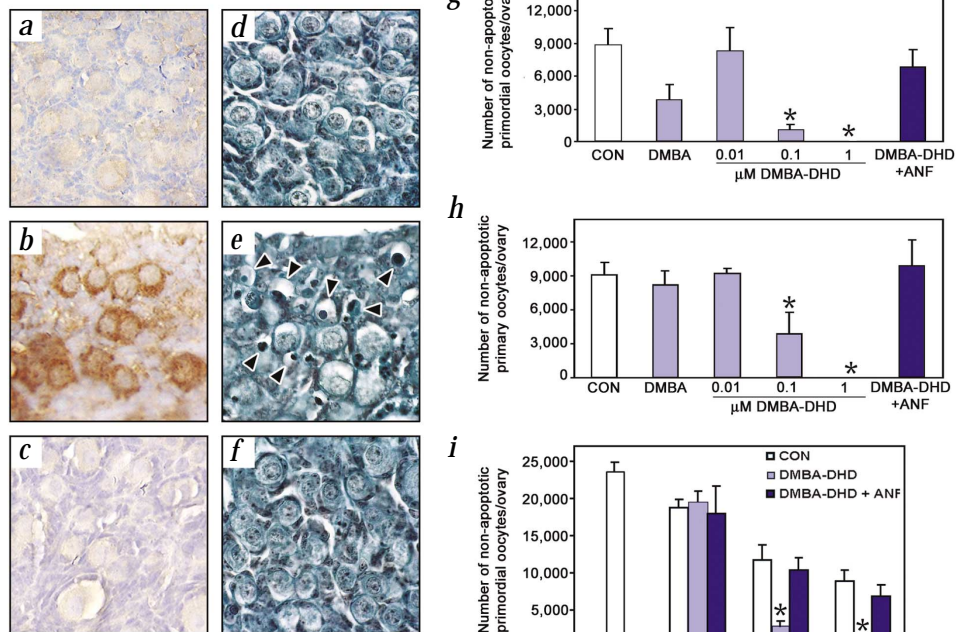


Fig. 1 Identification of *Bax* as a candidate target gene for the PAH-activated Ahr. **a**, Location of two AHRE core sequences (underlined bold type) in the wildtype murine *Bax* promoter (nucleotide numbering corresponding to the first nucleotide of the translation start site being designated as +1). **b**, Sequence of the murine *Bax* promoter containing inactivating mutations (red text) in the AHREs ('AHRE-dead' *Bax* gene promoter). **c**, Sequence of the murine *Bax* promoter following site-directed mutagenesis of the third nucleotide downstream from each AHRE to adenine (red text) to generate a 'dioxin-responsive element'. **d**, Northern-blot analysis (data from four independent experiments shown) reveals elevated *Bax* mRNA levels in the ovaries of prepubertal wildtype female mice 24 h after a single intraperitoneal injection of DMBA (50 mg/kg body weight) compared with those levels in vehicle-treated ovaries. Following normalization against the 18S rRNA level in each sample, the *Bax* mRNA level is increased 1.72±0.08-fold (mean±s.e.m, n=4, P=0.021) over vehicle-treated controls. **e–j**, Immunohistochemical analysis of *Bax* protein in mouse ovaries exposed to vehicle (**e, g, i**) or DMBA (**f, h, j**) for 24 h, as described above, shows a marked accumulation of *Bax* protein (brown staining) in primordial and primary oocytes (arrowheads) following PAH treatment compared with vehicle-treated controls (representative of results from four independent experiments). We selected the dose of DMBA based on previous work with C57BL/6 female mice reporting the nearly complete destruction of oocyte-containing primordial follicles by 5–6 d post-injection³⁰.

¹Vincent Center for Reproductive Biology, Department of Obstetrics and Gynecology, Massachusetts General Hospital/Harvard Medical School, Boston, Massachusetts 02114, USA. ²Samuel Lunenfeld Research Institute, Mount Sinai Hospital, Toronto, Ontario M5G 1X5, Canada. ³Department of Environmental Health, Boston University Schools of Medicine and Public Health, Boston, Massachusetts 02118, USA. ⁴Division of Immunology, Beth Israel Deaconess Medical Center/Harvard Medical School, Boston, Massachusetts 02115, USA. ⁵Department of Preventive Medicine, Kyoto Prefectural University School of Medicine, Kyoto 602-8566, Japan. ⁶Howard Hughes Medical Institute, Departments of Pathology and Medicine, Dana-Farber Cancer Institute/Harvard Medical School, Boston, Massachusetts 02115, USA. Correspondence should be addressed to J.L.T. (e-mail: jtilly@partners.org).

letter

Fig. 2 PAH-driven Bax protein accumulation and apoptosis in oocytes is Ahr antagonist-sensitive. **a–c**, Immunohistochemical analysis of Bax protein (brown staining) in neonatal mouse ovaries following a 24-h *ex vivo* treatment with vehicle (**a**), 0.1 μ M DMBA-DHD (**b**) or 0.1 μ M DMBA-DHD plus 1 μ M α -naphthoflavone (ANF) (**c**). Note that PAH-induced Bax production (**b**) is prevented by the Ahr antagonist ANF (**c**). This induction of Bax protein is not observed at an earlier time point (12 h) following PAH exposure (data not shown). **d–f**, Histological analysis of ovaries treated for 48 h as described in panels **a–c**, respectively, reveals that oocyte apoptosis resulting from PAH treatment (arrowheads in panel **e**) is, like Bax production, suppressed by ANF (**f**). **g, h**, Number of non-apoptotic oocyte-containing primordial (**g**) and primary (**h**) follicles remaining in ovaries exposed *ex vivo* for 72 h to vehicle (control, CON), DMBA (1 μ M), DMBA-DHD (0.01–1.00 μ M) or DMBA-DHD (0.1 μ M) plus ANF (1 μ M). These data show the dose-dependent nature of the oocyte destruction caused by DMBA-DHD, the potency difference between the parent compound (DMBA) and its Cyp1b1-derived metabolite (DMBA-DHD), and the effectiveness of ANF in preventing PAH-induced oocyte loss. Based on results from a time-course analysis of primordial oocyte destruction resulting from exposure to 0.1 μ M DMBA-DHD (**i**), the increase in Bax production (**b**) was determined to precede oocyte apoptosis. Panels **a–f** are representative of the results obtained from three independent experiments, whereas panels **g–i** are the mean \pm s.e.m. of combined data from at least three independent experiments (* P <0.05 versus respective control).



As apoptosis is the principal mechanism by which oocyte depletion is mediated under both normal conditions and as a pathologic response to anticancer therapies^{7–11}, we hypothesized that genes involved in the regulation of cell death would be prime targets for transcriptional regulation by the PAH-activated Ahr in female germ cells. After computer-based scanning of the promoter sequences of a number of apoptosis regulatory genes, we discovered two core Ahr response elements (AHREs) in the mouse *Bax* promoter (Fig. 1a). That this key proapoptotic gene is transactivated in oocytes by the Ahr is supported by findings that a single intraperitoneal injection of 9,10-dimethylbenz[*a*]anthracene (DMBA), a prototypical PAH, significantly increases ovarian *Bax* mRNA levels (Fig. 1d), with a corresponding accumulation of Bax protein in quiescent (primordial) and early growing (primary)

oocytes (Fig. 1e–f). Since both the Ahr¹² and its dimerization partner, the Ahr nuclear translocator (data not shown; see Methods), are expressed in oocytes, these results raised the possibility that *Bax* is directly regulated by the PAH-activated Ahr.

Previous studies have reported that the ovary is capable of metabolizing parent PAH compounds, such as DMBA, to biologically active intermediates¹³. We therefore first clarified whether a DMBA metabolite, as opposed to or in addition to DMBA, triggers Ahr activation leading to *Bax* gene expression and apoptosis in oocytes, by culturing neonatal mouse ovaries *ex vivo* without or with DMBA, or with its P450CYP1B1-derived early metabolite, DMBA-3,4-dihydrodiol (DMBA-DHD)¹⁴. Ovaries cultured with vehicle showed negligible Bax production (Fig. 2a) and cell death (Fig. 2d,g–i); however, both DMBA and DMBA-DHD induce Bax accumulation (Fig. 2b) and apoptosis (Fig. 2e,g–i) in primordial and primary oocytes, as the metabolite is one log order more potent in initiating germ cell destruction (Fig. 2g,h). Co-treatment with the Ahr antagonist α -naphthoflavone (ANF)¹⁵ inhibits both Bax production and oocyte death resulting from DMBA-DHD exposure (Fig. 2c,f,g–i). These results were reinforced by findings that the toxic responses of wildtype ovaries to DMBA-DHD (Fig. 2b,e,g–i) are similarly absent in the ovaries of *Ahr*^{-/-} mice

Table 1 • Induction of human oocyte apoptosis following PAH exposure *in vivo*

Days post-DMBA exposure	Incidence of oocyte death		Number of sections/grfts analyzed		
	Primordial stage	Primary stage			
1	0/15 (0%)	0/24 (0%)	133/4		
2	0/33 (0%)	31/72 (43%)	139/4		
3	4/43 (9%)	16/41 (39%)	100/4		
6	33/43 (76%)	7/10 (70%)	156/6		
DMBA dose (mg/kg bw)	Incidence of oocyte death		Number of sections/grfts analyzed		
	Primordial stage	Primary stage			
	0	2/35 (6%)		0/24 (0%)	141/6
	10	11/105 (11%)		36/86 (42%)	218/6
50	33/43 (76%)	7/10 (70%)	156/6		

For the time-course study, we used a DMBA dose of 50 mg/kg body weight (bw), based on previous dose–response data for DMBA-induced oocyte destruction in female mice³⁰. For the DMBA dose–curve study, we removed grfts for oocyte counts at 6 d post-injection. Both data sets are presented as the number of dying or dead oocytes (see Fig. 6i–l) at either the resting (primordial) or early growing (primary) stage of development per total number of oocytes scored; the mean percentage value is provided in parentheses. The total number of sections and grfts analyzed for each group is also provided.

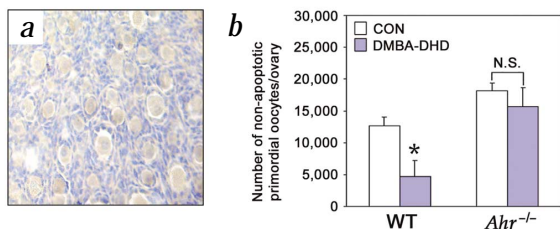


Fig. 3 The Ahr is required for PAH-initiated oocyte destruction. In contrast to the toxic responses of wildtype (WT) ovaries to DMBA-DHD (Bax expression: Fig. 2*b*; oocyte loss: panel *b*; see also Fig. 2*e,g-i*), the ovaries of *Ahr*^{-/-} mice do not show increased Bax production (*a*; 24 h after PAH exposure) or oocyte destruction (*b*; 48 h after PAH exposure) following treatment with 0.1 μ M DMBA-DHD. Panel *a* is representative of the results obtained in three independent experiments, whereas panel *b* is the mean \pm s.e.m. of combined data from 3–4 independent experiments (* $P=0.004$ versus vehicle control, CON; N.S., not significantly different).

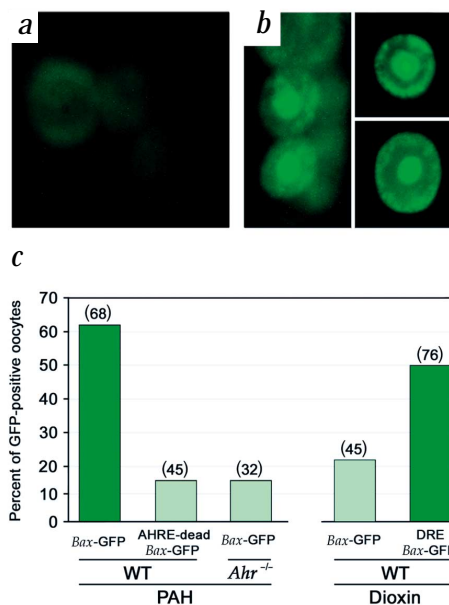
treated in parallel (Fig. 3). Since DMBA-DHD is known to bind with and activate the Ahr¹⁶, these data collectively indicate that the Ahr is functionally required for PAHs to induce *Bax* expression and apoptosis in oocytes.

To test whether PAH-induced oocyte loss is causally related to increased *Bax* expression, we prepared a *Bax* promoter–green fluorescent protein (GFP) reporter construct that was microinjected into oocytes for single-cell evaluation of *Bax* transcription. As with controls, GFP expression was not detected following the PAH treatment of oocytes microinjected with the GFP vector lacking the *Bax* promoter, or following the vehicle treatment of oocytes microinjected with the *Bax* promoter–GFP construct (Fig. 4*a*; quantitative data not shown). In contrast, 62% of wildtype oocytes microinjected with the *Bax* promoter–GFP construct, and then treated with PAHs, exhibited a high level of GFP protein (Fig. 4*b,c*). In comparison, only 16% of wildtype oocytes microinjected with a *Bax* promoter in which the tandem AHRE gene sequences were mutated (Fig. 1*b*; AHRE-dead) produced GFP following PAH exposure in parallel (Fig. 4*c*). Similarly, only 16% of *Ahr*-deficient oocytes microinjected with the wildtype *Bax* promoter–GFP construct showed GFP production after PAH treatment (Fig. 4*c*). To test whether the end product of PAH-induced *Bax* gene transcription (that is, Bax protein) is necessary for the apoptotic response, we compared the effects of PAHs in the ovaries of wildtype and *Bax*-deficient mice. These experiments show that the massive oocyte destruction observed in wildtype ovaries exposed to PAHs (Fig. 2*b,e,g-i*) is entirely absent in ovaries of *Bax*^{-/-} mice treated in parallel (Fig. 5*a*). Thus, Ahr-driven *Bax* expression represents a novel apoptosis-signaling mechanism, and activation of this pathway is functionally required for oocyte loss caused by exposure to PAHs.

Fig. 4 PAH-driven *Bax* transcription requires functional AHREs and Ahr. **a,b**, Expression of GFP in wildtype oocytes microinjected with a wildtype *Bax* promoter–GFP reporter construct is observed after exposure to 1 μ M DMBA-DHD (*b*) but not to vehicle (*a*). **c**, Quantitative analysis of the percentage of GFP-positive wildtype (WT) oocytes microinjected with the wildtype *Bax* promoter–GFP construct (*Bax*-GFP), or with the mutant *Bax* promoter–GFP construct in which both AHREs were inactivated (AHRE-dead *Bax*-GFP; see Fig. 1*b*), following DMBA-DHD exposure. The latter findings underscore the importance of the AHRE to PAH-induced *Bax* expression. The functional requirement of the Ahr for PAHs to induce *Bax* expression is shown by the blunted GFP response of *Ahr*^{-/-} oocytes, microinjected with the wildtype *Bax* promoter–GFP construct, to DMBA-DHD treatment. Unlike PAHs, dioxin (doses of 0.001–1.000 μ M tested with similar results, 0.1 μ M dose shown) is a relatively poor activator of the wildtype *Bax* promoter. However, by changing only the third nucleotide downstream of each core AHRE to adenine (dioxin-responsive element or DRE *Bax*-GFP; see Fig. 1*c*), the mutated *Bax* promoter acquires sensitivity to dioxin (0.1 μ M)-driven transcriptional activation. The total number of oocytes microinjected in each group is indicated in parentheses over the respective bar. Panels *a* and *b* are representative of results obtained from at least three independent experiments.

In contrast to the cytotoxic effects of PAHs in oocytes, dioxin (2,3,7,8-tetrachlorodibenzo-*p*-dioxin), a halogenated biphenyl that binds and activates the Ahr with high affinity^{4,5}, does not induce oocyte destruction^{13,17}. This marked difference in tissue response to PAHs versus dioxin, which is not restricted to oocytes (being seen in, for example, lymphocytes¹⁶), has for years remained an enigma in the Ahr field. In the ovary, the disparity between the response of oocytes to PAHs and to dioxin is further complicated by the fact that dioxin, like PAHs, is a potent stimulator of ovarian P450 metabolic enzyme activity^{13,17}. In light of the data presented above, one possible explanation for why oocytes die in response to PAHs, but not dioxin, is that the dioxin-activated Ahr is unable to effectively induce the *Bax* expression required for oocyte apoptosis. In support of this, we found that only 22% of wildtype oocytes microinjected with the *Bax* promoter–GFP construct and treated with dioxin were GFP positive (Fig. 4*c*). This low level of induction is comparable to that observed in PAH-treated wildtype oocytes microinjected with the AHRE-dead *Bax* promoter–GFP construct, or in PAH-treated *Ahr*-deficient oocytes microinjected with the wildtype *Bax* promoter–GFP construct (Fig. 4*c*). Previous studies of the *Cyp1a1* promoter have shown that the third base downstream of the 'core' five nucleotide AHRE sequence (5'–GCGTG–3') must be an adenine (5'–GCGTGNN_A–3') for the dioxin-activated Ahr to be functional in a transcriptional reporter assay^{18,19}. As further examination of the *Bax* promoter (Fig. 1*a*) revealed that the third base downstream of the core AHRE was a guanine (AHRE 1) or a cytosine (AHRE 2), we tested whether this single base-pair sequence conveys specificity for *Bax* transcription modulated by different Ahr ligands. After site-directed mutagenesis to change the third nucleotide downstream of both core AHREs in the *Bax* promoter to adenine (Fig. 1*c*), dioxin now effectively induces activation of the mutated *Bax* promoter in microinjected oocytes (Fig. 4*c*). These data provide the first mechanistic insight into how these two different ligands for the Ahr can lead to different patterns of gene expression in the same cell and, in the case of the oocytes, why dioxin is not cytotoxic.

Finally, sequence analysis of the human *Bax* promoter indicates the presence of 4 core AHREs, 3 of which lie within 700 bp of each other (data not shown). We therefore employed a human



letter

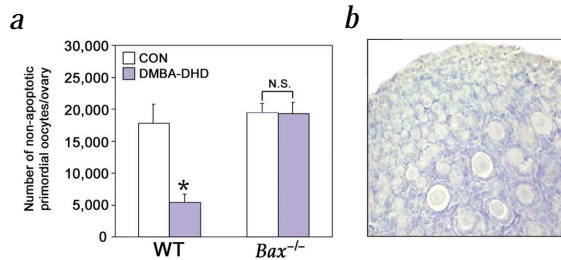


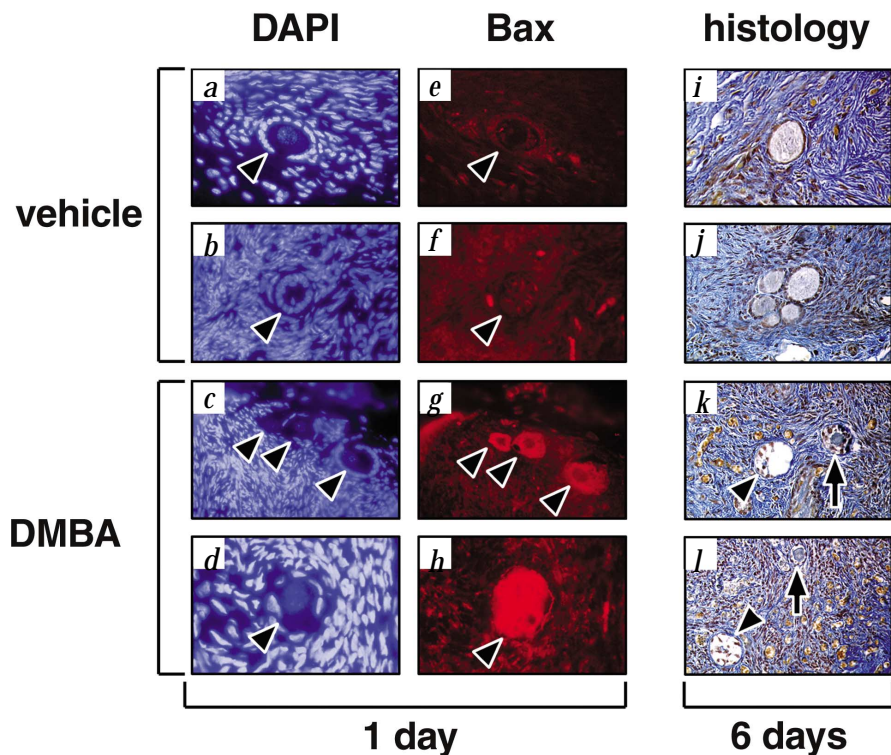
Fig. 5 *Bax* is required for PAH-induced oocyte destruction. The ovaries of *Bax*^{-/-} mice do not exhibit oocyte destruction (**a**: 48 h after PAH exposure) following treatment with 0.1 μ M DMBA-DHD, in contrast to the loss of oocytes in wild-type (WT) ovaries exposed to DMBA-DHD (**a**; see also Fig. 2*e,g-f*). Specificity of the *Bax* immunostaining (Fig. 1*e-j*, Fig. 2*a-c* and Fig. 3*a*) is shown by the absence of an immunoreaction in *Bax*-deficient ovaries analyzed in parallel (**b**). Panel **a** is the mean \pm s.e.m. of combined data from 3–4 independent experiments (* $P=0.02$ versus vehicle control, CON; N.S., not significantly different), whereas panel **b** is representative of the results obtained from three independent experiments.

ovarian xenograft model to determine whether a similar mechanism could be responsible for the ovarian damage presumed to occur in human females following PAH exposure *in vivo*. Immunodeficient mice containing subcutaneously grafted human ovarian cortical tissue fragments were given single intraperitoneal injections of vehicle or increasing concentrations of DMBA. Between one and six days after *in vivo* treatment, we excised the grafts for an assessment of *Bax* production and oocyte death. As in mouse ovaries, the level of *Bax* was low or undetectable in the primordial and primary oocytes of vehicle-treated human ovaries (Fig. 5*a,b,e,f*). A pronounced increase in *Bax* accumulation occurred, however, in human primordial and primary oocytes within 24 hours of PAH exposure *in vivo* (Fig. 5*c,d,g,h*), followed by a striking increase in the incidence of degenerating oocytes throughout the grafted human ovarian tissues (Fig. 5*i-l*). The *in vivo* destruction of human oocytes by PAHs was found to be time and dose dependent (Table 1). In fact, 6 days following injection of the highest dose of DMBA, approximately 70% of the primordial and primary oocytes had degenerated in response to PAH exposure, compared with only 6% or fewer dying or dead oocytes in the vehicle controls (Table 1). These findings provide the first direct evidence that PAHs induce human oocyte death *in vivo* and that this oocyte loss, like that in mice, is associated with an accumulation of *Bax* protein.

In conclusion, we have identified a new intracellular cell-death signaling pathway, and have shown that the activation of this pathway by DMBA, a member of a ubiquitous class of toxic environmental chemicals, can cause oocyte loss and

ovarian failure. That the PAH-activated Ahr leads to oocyte death through increased *Bax* expression is supported not only by the finding that *Bax*-deficient oocytes are resistant to PAH-induced apoptosis, but also by the fact that the *Bax* promoter is relatively insensitive to dioxin, an Ahr ligand that does not induce oocyte destruction. These data, along with recent observations that the microinjection of recombinant *Bax* protein into oocytes directly induces apoptosis¹⁰, indicate that an elevated level of *Bax* is both necessary and sufficient to trigger female germ cell death. Furthermore, our finding that a single nucleotide flanking the core AHRE sequence determines the transcriptional sensitivity of a given gene to the PAH- versus dioxin-activated Ahr offers a new mechanistic insight into how two different ligands for the same transcription factor elicit completely different genomic responses in the same cell lineage. Finally, immunodeficient mice housing grafted human gonadal tissue provide a long sought-after model, which accounts for the route of exposure and metabolism, to conduct mechanistic studies and risk assessments of putative biohazards and new drugs for human reproductive toxicity *in vivo*. Indeed, the data derived from use of this model strongly support the contention that the early onset of menopause in women smokers^{1,3} is caused, at least in part, by the proapoptotic actions of tobacco smoke-derived PAHs in human oocytes.

Fig. 6 PAHs induce *Bax* production and apoptosis in human oocytes *in vivo*. **a-h**, Immunohistochemical analysis of *Bax* protein levels in oocytes (arrowheads) within human ovarian grafts 24 h after exposure, *in vivo*, to vehicle (**e,f**) or 50 mg/kg DMBA (**g,h**). Following antigen detection using Texas red indirect immunofluorescence (**e-h**), nuclear counterstaining was performed with the DNA-binding dye, 4',6-diamidino-2-phenylindole (DAPI; **a-d**). **i-l**, Morphological analysis of oocyte-containing follicles in human ovarian grafts 6 d after a single injection of vehicle (**i,j**) or 50 mg/kg DMBA (**k,l**). Oocytes within the follicles of human ovarian grafts exposed to PAH *in vivo* (**k,l**) have degenerated (arrowheads) or are in the process of condensation (arrows), whereas oocytes within the follicles of human ovarian grafts exposed to vehicle (**i,j**) exhibit a normal healthy appearance. Quantitative results from these experiments are presented in Table 1.





Methods

Mice. We obtained wildtype C57BL/6 female mice from Charles River Laboratories. We used heterozygous *Ahr* (*Ahr*^{+/-}) male and female mice (C57BL/6-*Ahr*^{tm1Bra}), obtained from Jackson Laboratories, to generate wildtype and *Ahr*-deficient female littermates for the direct comparison of ovarian or oocyte responses to PAHs (Figs. 3 and 4, respectively). We backcrossed the original *Bax* mutant mouse line²⁰ onto a congenic background of C57BL/6 and then used heterozygous (*Bax*^{+/-}) male and female mice to generate wildtype and *Bax*-deficient female littermates for a direct comparison of the ovarian responses to PAHs (Fig. 5). All animal work was conducted using protocols approved by Institutional Animal Care and Use Committees of the Massachusetts General Hospital, Boston University School of Medicine and University of Toronto.

Ovarian organ cultures. We collected ovaries from day 4 post-partum female mice and fixed the ovaries immediately or after serum-free organ culture²¹ for 24, 48 or 72 h with vehicle, DMBA (1 μM) or DMBA-DHD (0.01–1.00 μM) in the absence or presence of 1 μM ANF. We then processed the ovaries for the histomorphometric analysis of the number of nonapoptotic oocytes present in quiescent (primordial) and early growing (primary) follicles^{8–10,22} or for immunohistochemical analysis of the *Bax* protein level (see Gene expression analysis).

Gene expression analysis. We generated a partial complementary DNA, corresponding to bases 107–508 of the mouse *Bax* coding sequence (GenBank accession number L22472), by RT-PCR²³ using total RNA isolated from adult mouse ovaries, and subcloned this cDNA into the pGEM4z vector (Promega). Following sequence analysis to confirm its identity, we then used this cDNA to prepare a radiolabeled antisense RNA probe for northern-blot analysis of *Bax* messenger RNA transcripts in total RNA samples (5 μg/lane), as described²³. To control for equality of RNA sample loading, we rehybridized the blots with a radiolabeled probe against 18S ribosomal RNA (Ambion), as described²⁴. Following the densitometric scanning of hybridization signal intensities, we normalized the levels of *Bax* mRNA in each sample against the respective levels of 18S rRNA prior to data analysis. For assessment of the *Bax* protein level, we immunostained paraformaldehyde-fixed, paraffin-embedded tissue sections using a 1:50 dilution of an affinity-purified rabbit polyclonal antibody raised against mouse *Bax* (P-19; Santa Cruz Biotechnology) after high-temperature antigen unmasking²⁵, followed by antigen detection using diaminobenzidine or Texas red. We always processed vehicle- and PAH-treated ovaries in parallel, and we confirmed the specificity of the immunostaining conditions using *Bax*-deficient ovaries as a negative control (Fig. 5b). We determined the expression of the *Ahr* nuclear translocator in oocytes by subjecting the total RNA extracted from mouse immature oocytes to RT-PCR amplification²⁶, using oligonucleotide primers corresponding to bases 1995–2015 (forward primer) and 2408–2427 (reverse primer) of the *Ahr* nuclear translocator cDNA coding sequence (GenBank accession number U10325). We confirmed the identity of the 424-bp amplified product by restriction enzyme mapping and sequence analysis.

Promoter analysis and site-directed mutagenesis. We first ligated a fragment of the mouse *Bax* promoter²⁷, corresponding to bases –22 to –2694 (the first base of the translation start site being designated as +1), upstream of the coding sequence for GFP in the pBlueScript-KS vector (Stratagene). We then isolated immature (germinal-vesicle stage) oocytes enclosed within 1–2 layers of granulosa cells from the ovaries of wildtype or *Ahr*^{+/-} mice at day 12 postpartum by mechanical dissection over a 60–90 min period using 26-gauge needles under a dissecting microscope²⁸. Once they had been isolated, we microinjected the oocytes with the parent GFP vector (lacking the *Bax* promoter) or the *Bax* promoter–GFP construct (600 fg DNA per oocyte; 60–70 oocytes within 60 min) and discarded those oocytes that did not survive the microinjection procedure (routinely <25%). We cultured the remaining oocytes in the absence (vehicle) or presence of 1 μM DMBA-DHD for 6–18 h, and assessed GFP production by fluorescence microscopy. We obtained similar results if fully denuded immature oocytes (that is, those free of adherent granulosa cells) were used to assess the effects of PAH on *Bax* promoter activity (data not shown).

We performed inactivating mutations of the AHREs using the QuikChange™ Site-Directed Mutagenesis kit (Stratagene), with primers containing two base-pair mutations in each of the AHREs (GAATG and

CAAAC in AHRE1 and AHRE2, respectively; compare Fig. 1b with the wildtype AHRE sequences in Fig. 1a). We performed point mutations in the sequences flanking the AHREs as described above using primers containing a single base-pair mutation at the third nucleotide downstream of each AHRE (compare Fig. 1c with the wildtype AHRE-flanking sequences in Fig. 1a).

Human ovarian xenografts. We collected human ovarian tissue from three patients (33, 34 and 40 years of age, ovarian tissue from each patient representing a single experiment) undergoing gynecologic surgery for benign conditions, after informed consent and approval from the Mount Sinai Hospital institutional review board. We then subcutaneously grafted a total of 55 ovarian cortical biopsies (each 1–2 mm²) into NOD-SCID mice (n=37, with 1–2 grafts per mouse) through small dorsomedian transverse incisions above the flank²⁹. After 2–3 weeks, to allow the grafts to become vascularized, we gave the mice a single intraperitoneal injection of vehicle (paraffin oil) or DMBA (10 or 50 mg/kg dissolved in paraffin oil) and removed the grafts at 1, 2, 3 or 6 d post-injection. After fixation, we analyzed each graft for the number of degenerating or dead oocyte-containing primordial and primary follicles (out of the total number of oocytes at each stage present in the grafted tissue) or for the *Bax* protein level (see sections on Ovarian organ cultures and Gene expression analysis, respectively).

Acknowledgments

We thank K.I. Tilly, X.-J. Tao and T. Manganaro for technical help, S. Riley for assistance with the image analysis, and I. Schiff for critical reading of the manuscript. This study was supported by the National Institutes of Health (R01-ES08430), the Canadian Toxic Substances Research Initiative, the Harvard Center of Excellence in Women's Health, and Vincent Memorial Research Funds. We conducted this work while T.M. and J.L. were Research Fellows supported by the Finnish Foundation for Pediatric Research and the Finnish Cultural Foundation. A.J. was a Research Fellow supported by the Canadian Institutes of Health Research, and J.K.P. was a Research Fellow supported by the Lalor Foundation.

Received 26 January; accepted 25 May 2001.

- Mattison, D.R. *et al.* The effect of smoking on oogenesis, fertilization and implantation. *Sem. Reprod. Health* **7**, 291–304 (1989).
- Sussman, N.B., Mazumdar, S. & Mattison, D.R. Modeling adverse environmental impacts on the reproductive system. *J. Women's Health* **8**, 217–226 (1999).
- Jick, H. & Porter, J. Relation between smoking and age of natural menopause. Report from the Boston Collaborative Drug Surveillance Program, Boston University Medical Center. *Lancet* **1**, 1354–1355 (1977).
- Hankinson, O. The aryl hydrocarbon receptor complex. *Ann. Rev. Pharmacol. Toxicol.* **35**, 307–340 (1995).
- Wilson, C.L. & Safe, S. Mechanisms of ligand-induced aryl hydrocarbon receptor-mediated biochemical and toxic responses. *Toxicol. Pathol.* **26**, 657–671 (1998).
- Oltvai, Z.N., Milliman, C.L. & Korsmeyer, S.J. Bcl-2 heterodimerizes *in vivo* with a conserved homolog, *Bax*, that accelerates programmed cell death. *Cell* **74**, 609–619 (1993).
- Morita, Y. & Tilly, J.L. Oocyte apoptosis: like sand through an hourglass. *Dev. Biol.* **213**, 1–17 (1999).
- Perez, G.I., Knudson, C.M., Leykin, L., Korsmeyer, S.J. & Tilly, J.L. Apoptosis-associated signaling pathways are required for chemotherapy-mediated female germ cell destruction. *Nature Med.* **3**, 1228–1232 (1997).
- Perez, G.I. *et al.* Prolongation of ovarian lifespan into advanced chronological age by *Bax*-deficiency. *Nature Genet.* **21**, 200–203 (1999).
- Morita, Y. *et al.* Oocyte apoptosis is suppressed by disruption of the *acid sphingomyelinase* gene or by sphingosine-1-phosphate therapy. *Nature Med.* **6**, 1109–1114 (2000).
- Pru, J.K. & Tilly, J.L. Programmed cell death in the ovary: insights and future prospects using genetic technologies. *Mol. Endocrinol.* **15**, 845–853 (2001).
- Robles, R. *et al.* The aryl hydrocarbon receptor, a basic helix-loop-helix transcription factor of the PAS gene family, is required for normal ovarian germ cell dynamics in the mouse. *Endocrinology* **141**, 450–453 (2000).
- Mattison, D.R. & Nightingale, M.R. The biochemical and genetic characteristics of murine ovarian aryl hydrocarbon (benzo[*a*]pyrene) hydroxylase activity and its relationship to primordial oocyte destruction by polycyclic aromatic hydrocarbons. *Toxicol. Appl. Pharmacol.* **56**, 399–408 (1980).
- Heidel, S.M., Czuprynski, C.J. & Jefcoate, C.R. Bone marrow stromal cells constitutively express high levels of cytochrome P4501B1 that metabolize 7,12-dimethylbenz[*a*]anthracene. *Mol. Pharmacol.* **54**, 1000–1006 (1998).
- Blank, J.A., Tucker, A.N., Sweatlock, J., Gasiewicz, T.A. & Luster, M.I. α -Naphthoflavone antagonism of 2,3,7,8-tetrachlorodibenzo-*p*-dioxin-induced murine lymphocyte ethoxyresorufin-O-deethylase activity and immunosuppression. *Mol. Pharmacol.* **32**, 169–172 (1987).
- Mann, K.K. *et al.* The role of polycyclic aromatic hydrocarbon metabolism in dimethylbenz[*a*]anthracene-induced pre-B lymphocyte apoptosis. *Toxicol. Appl. Pharmacol.* **161**, 10–22 (1999).
- Silbergeld, E.K. & Mattison, D.R. Experimental and clinical studies on the reproductive toxicology of 2,3,7,8-tetrachlorodibenzo-*p*-dioxin. *Am. J. Ind. Med.* **11**, 131–144 (1987).
- Shen, E.S. & Whitlock Jr., J.P. Protein-DNA interactions at a dioxin-responsive enhancer. Mutational analysis of the DNA-binding site for the liganded Ah receptor. *J. Biol. Chem.* **267**, 6815–6819 (1992).



letter

19. Lusska, A., Shen, E. & Whitlock Jr., J. P. Protein-DNA interactions at a dioxin-responsive enhancer. Analysis of six *bona fide* DNA-binding sites for the liganded Ah receptor. *J. Biol. Chem.* **268**, 6575–6580 (1993).
20. Knudson, C.M., Tung, K.S., Tourtellotte, W.G., Brown, G.A. & Korsmeyer, S.J. Bax-deficient mice with lymphoid hyperplasia and male germ cell death. *Science* **270**, 96–99 (1995).
21. Eppig, J.J. & O'Brien, M.J. Development *in vitro* of mouse oocytes from primordial follicles. *Biol. Reprod.* **54**, 197–207 (1996).
22. Morita, Y., Perez, G.I., Maravei, D.V., Tilly, K.I. & Tilly, J.L. Targeted expression of Bcl-2 in mouse oocytes inhibits ovarian follicle atresia and prevents spontaneous and chemotherapy-induced oocyte apoptosis *in vitro*. *Mol. Endocrinol.* **13**, 841–850 (1999).
23. Tilly, J.L., Tilly, K.I., Kenton, M.L. & Johnson, A.L. Expression of members of the *bcl-2* gene family in the immature rat ovary: equine chorionic gonadotropin-mediated inhibition of granulosa cell apoptosis is associated with decreased *bax* and constitutive *bcl-2* and *bcl-x_{long}* messenger RNA levels. *Endocrinology* **136**, 232–241 (1995).
24. Pru, J. K. *et al.* Interferon-tau suppresses prostaglandin-F_{2α} secretion independently of the mitogen-activated protein kinase and nuclear factor-κB pathways. *Biol. Reprod.* **64**, 965–973 (2001).
25. Shi, S.R., Cote, R.J. & Taylor, C.R. Antigen retrieval immunohistochemistry: past, present, and future. *J. Histochem. Cytochem.* **45**, 327–343 (1991).
26. Jurisicova, A., Latham, K.E., Casper, R.F. & Varmuza, S.L. Expression and regulation of genes associated with cell death during murine preimplantation embryo development. *Mol. Reprod. Dev.* **51**, 243–253 (1998).
27. Igata, E. *et al.* Molecular cloning and functional analysis of the murine *bax* gene promoter. *Gene* **238**, 407–415 (1999).
28. Ovist, R., Blackwell, L.F., Bourne, H. & Brown, J.B. Development of mouse ovarian follicles from primary to preovulatory stages *in vitro*. *J. Reprod. Fertil.* **89**, 169–180 (1990).
29. Weissman, A. *et al.* Preliminary experience with subcutaneous human ovarian cortex transplantation in the NOD-SCID mouse. *Biol. Reprod.* **60**, 1462–1467 (1999).
30. Mattison, D.R. & Thorgeirsson, S.S. Ovarian aryl hydrocarbon hydroxylase activity and primordial oocyte toxicity of polycyclic aromatic hydrocarbons in mice. *Cancer Res.* **39**, 3471–3475 (1979).